OCEANOLOGIA, 26, 1988
PL ISSN 0078-3234

Atmosphere-ocean interaction
Momentum transfer
Low-frequency wave

Role of low-frequency water waves on momentum transfers between atmosphere and ocean in the near shore region

JANUSZ KRZYŚCIN
Institute of Geophysics,
Polish Academy of Sciences,
Warszawa

Manuscript received February 19, 1987, in final form December 28, 1987.

Abstract

Using the Gent and Taylor model, the calculations of modifications of an interaction between atmosphere and ocean near coastal shore region by low frequency ocean surface waves were made. Model equations consist of the wave kinematics equations and the wave energy equation. In the latter equation sources of energy (wind, surface water current) and energy dissipation by sea bottom were parameterized. The model equations were used to find changes of the long waves in the near shore region. The method of numerical calculations is based on the method of characteristics.

Results show that significant changes of the drag coefficient for momentum are caused by the waves propagating opposite to the local wind. When waves are generated by local wind (direction of the long wave is along the wind) the drag coefficient is mainly connected with high frequency surface waves. A type of the sea bottom material and surface current modify propagation of the long wave. These induce appriopriate changes of the drag coefficient in the near shore region.

1. Introduction

The sea-atmosphere interface consists of moving irregularities of various frequency. Within the high-frequency range of the wind generated waves phase velocity is considerable lower than wind velocity at a standard level of 10 m. When the wind begins to blow, these components of the wavy surface are generated immediately and can be found in higher stages of wind wave development. Capillary waves and short gravity waves belong to this wave category. When the wind duration is long enough, fast long gravity waves appear. Phase velocities of these waves are comparable to the wind velocity so surface irregularities cannot effectively slow down wind velocity near surface, as high frequency, nearly stationary, elements do. One can intuitively say that among various wave components, observed in developing surface water waves, mainly waves from a high-frequency band are responsible for the effective roughness of the free surface of the sea. An air flow over roughness elements is modified by long surface gravity waves so these frequency bands can play a specific role in the air-sea momentum transfer. This role is enhanced in processes which lead to flow separation, and during swell propagation against wind.

Munk (1955) first recognized an importance of the high-frequency band for sea-air momentum exchange processes. He used water waves energy density spectrum $S(\omega)$ to characterize random wave field. The standard deviation σ_0 of the ocean surface displacement is related to $S(\omega)$ as follow:

$$\sigma_0^2 = \int_0^\infty S(\omega)\,\mathrm{d}\,\omega. \tag{1}$$

Munk suggested that waves steepness is an important parameter characterizing the interaction between atmosphere and ocean. For the wave of an amplitude a and wave number k steepness is equal to $a \cdot k$. Mean steepness of the wavy surface $\nabla\sigma$ is calculated as a square root from integral of wave elementary steepnesses $a \cdot k$ raised to the second power. If we replace a^2 by wave energy spectrum we have finally:

$$(\nabla\sigma)^2 = \int_0^\infty S(\omega)\,k^2\,\mathrm{d}\omega = g^{-2}\int_0^\infty S(\omega)\,\omega^4\,\mathrm{d}\omega, \tag{2}$$

where:
ω – wave frequency,
g – acceleration due to gravity,
k – wave number.
In second integral on r.h.s. dispersion relation for deep water zone is used.

High-frequency spectrum $S(\omega)$ can be parameterized as a power function ω^{-p}, where $p < 4$, so that the main contribution to the integral comes from higher frequencies. Field observations gave for instance $p = 3.7$ at an early stage of wave developing (Druet, Siwecki, 1984) and $p = 3.0$ in the area of small relative depth (Massel, Druet, 1980).

In different regions of the sea (deep water area or shallow water zone) and stages of the wave development energy density spectrum $S(\omega)$ is expressed by specific formulas so the short gravity waves may act differently in these situations.

Numerous field and theoretical investigations have been carried out to find how wavy surface modifies a structure of the atmosphere adjacent to the water.

Kitaigorodskii (1970) obtained an important result. He found that the logarithmic profile of the wind, *ie*:

$$U(z) = \frac{u_*}{\varkappa} - \ln\left(\frac{z}{z_0}\right), \tag{3}$$

where:
u_* – friction velocity,
$\varkappa$ – Karman's constant,
z_0 – roughness parameter,
is a good approximation for the wind blowing over undulating sea.
The roughness parameter z_0 in this formula depends on conditions upon wavy surface. According to Kitaigorodskii (1970) z_0 is determined mainly by the high-frequency band. Special formulas for different stages of wave development and aerodynamic structure of the surface (rough or smooth) are presented. These formulas require field observation to find a dimensionless function depending on parameters connected with low and high-frequency component of the surface irregularities.
Conclusions from field observations carried out by different authors were not the same. Kuznetsov (1978) found a relationship between the friction velocity and the root mean square deviation of the high-frequency irregularities, but Hasse *et al* (1978) pointed out the dependence u_* on global energy, mainly determined by long surface wave.

A theoretical model proposed by Gent and Taylor (1978) clarified the role of low- and high-frequency band of the surface wave spectrum in momentum transfer. In this model the authors calculated a characteristic of the flow over rough, long, surface gravity waves. Roughness of the surface was caused by small irregularities (high-frequency waves) allocated along basic low-frequency wave. A parameter z_0 was proportional to the mean height of the small irregularities. Interaction between atmosphere and ocean the authors described using a drag coefficient $C_{10} = (u_*/U_{10}^2)$.
Some of the results derived by Gent and Taylor are presented in Figures 1 and 2. From these pictures one can draw the following conclusions:

– exchange processes between sea and air are intensified when direction of the wave propagation is opposite to the near surface wind,

– steepness of the long wave $(a \cdot k)$ and ratio of its phase velocity to the friction velocity (c_f/u_*) are important parameters governing air-sea momentum transfer,

– deformation of the air flow by long surface wave plays a little role in exchange process – curve $C_s(z_0, a \cdot k)$ in Figure 2.

– when long wave is a wind driven wave, model using only parameter z_0 to determine C_{10} gives a good accuracy.

According to these conclusions the drag coefficient in a region of variable parameters of long low-frequency waves can also vary. A specific variability of the air-sea exchange processes in a near surface zone is expected, where parameters of the long waves change rapidly. Variability of the wave parameters and drag coefficient in this zone will be a subject of the present paper.

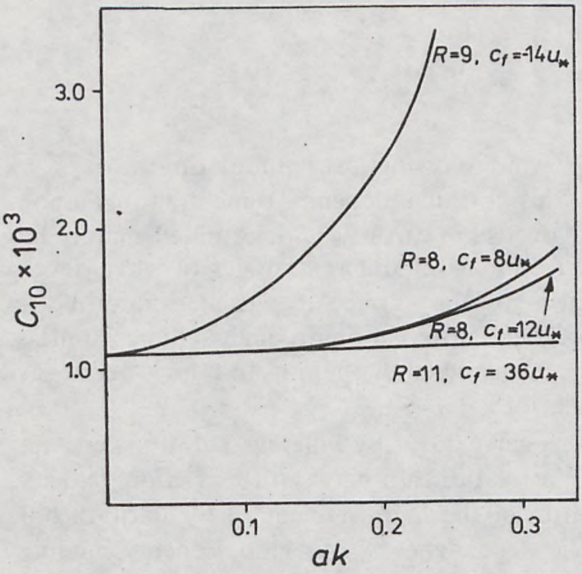

Fig. 1. Variations of the drag coefficient with wave slope for $z_0 = 0.005$ cm (after Gent, Taylor, 1978)

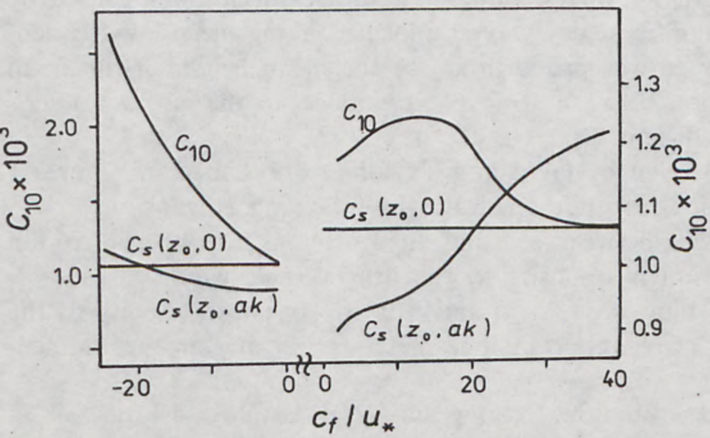

Fig. 2. Variation in C_{10}, $C_s(z_0, 0)$ (part of the drag coefficient C_{10} caused by small scale irregularities when gravity waves are absent), and $C_s(z_0, ak)$ (part of the drag coefficient caused by small scale irregularities superimposed on long gravity waves) with c_f/u_* (after Gent, Taylor, 1978)

2. Basic assumptions and equations of the model

According to Gent and Taylor, the drag coefficient depends on friction velocity and parameters of the long wave, *ie* wave-length (λ or wave number k), its amplitude (a) and group velocity (c_g). A constant roughness parameter z_0 is proportional to the square root of the energy of high-frequency components of wavy surface.

In the model presented the results derived by Gent and Taylor are adopted to the shallow water zone. Other parameters to express precisely variability of a near shore region are also included. The changes in long wave parameters are due to variations of surface current, water depth, and energy dissipation by bottom interaction effects (dissipation by friction, percolation, and bottom motion). Propagation of long surface waves is determined by wave kinematics equation in the form:

$$\frac{\partial}{\partial t}\vec{k}+\nabla(\omega+\vec{k}\cdot\vec{V}_p)=0, \tag{4}$$

where $\vec{k}$ is wave number vector ($|\vec{k}|=k$), $\vec{V}_p$ is velocity of the surface water current.
Equation (4) describes refraction of the long surface waves. Using dispersion relation $\omega^2 = gk \tanh(kd)$ – where d is water depth – and wave group definition $\vec{c}_g = \nabla_k \omega$, after some rearrangements we have:

$$\begin{aligned}
&\frac{\partial}{\partial t}k_x+(c_{gx}+U_p)\frac{\partial}{\partial x}k_x+(c_{gy}+V_p)\frac{\partial}{\partial y}k_x+k_x\frac{\partial}{\partial x}U_p+k_y\frac{\partial}{\partial x}V_p+\frac{\partial}{\partial d}\omega\frac{\partial}{\partial x}d=0,\\
&\frac{\partial}{\partial t}k_y+(c_{gx}+U_p)\frac{\partial}{\partial x}k_y+(c_{gy}+V_p)\frac{\partial}{\partial y}k_y+k_x\frac{\partial}{\partial y}U_p+k_y\frac{\partial}{\partial y}V_p+\frac{\partial}{\partial d}\omega\frac{\partial}{\partial y}d=0.
\end{aligned} \tag{5}$$

Wave energy (E) is defined as a sum of potential and kinetic energy of all water wavy fluctuations (orbital motion of elementary particles in the water) below and on the surface. For infinitesimal waves, potential theory of the surface waves gives $E = 0.5\,\varrho_w g\,\langle a^2\rangle$ either for deep water region or shallow water zone, where ϱ_w is a water density, $\langle a^2\rangle$ is a mean square height of surface irregularities. Wave energy equation in the form first given by Longuet-Higgins and Stewart (1961) is:

$$\frac{\partial}{\partial t}E+\frac{\partial}{\partial x}(c_{gx}+U_p)E+\frac{\partial}{\partial y}(c_{gy}+V_p)E=Z-D, \tag{6}$$

where Z and D denote sources and sinks of energy of water wavy fluctuations.
Energy transferred to the waves as a result of wind action in a unit of time is characterized by a dimensionless coefficient α,

$$\alpha = \frac{T}{\pi E}\frac{\mathrm{d}E}{\mathrm{d}t}, \tag{7}$$

where T is wave period of a dominant wave in a wave energy spectrum.

According to Gent (1977) α can be parameterized as:

$$\alpha = \frac{\varrho_\alpha u_*^2 k}{\varrho_w g}\mathrm{Gen}(R, \alpha k), \tag{8}$$

where:
ϱ_α – air density,
Gen – tabulated function,
$R = -\ln(kz_0)$.
Using equations (7) and (8) final expression of energy input from the wind is given by formula:

$$Z_{\mathrm{wind}} = 0.5\frac{\varrho_\alpha}{\varrho_w}\left(\frac{\hat{u}_*}{c_f}\right)^2 \omega \tanh(kd)\,\mathrm{Gen}(R, \alpha k)\,E. \tag{9}$$

In order to find values of Gen in intermediate points we used a linear interpolation between the values given by Gent (1977). An angle between direction of long waves propagation and wind is not constant. This effect is caused either by wind variability or wave refraction, so in equation (9) $\hat{u}_*^2$ represents projection of surface Reynolds stress (in the air) on direction of wave propagation.

Values of Z_{wind} need not be positive. In the case $Z_{\mathrm{wind}} < 0$ wave energy diminishes as a result of wind-wave interaction. This situation is met when swell propagates opposite to the local wind or during abrupt changes of meteorological fields (waves cannot adapt immediately to the local wind).

Dissipation mechanisms of the wave energy in a near shore region are connected with bottom friction, percolation within the sand layer, and wave motion in the mud layer induced by hydrodynamic forces acting at the mud line. A decay rate induced by these mechanisms depends strongly on the type of bottom sediments and grain diameter. Percolation is most effective in coarse sand (mean diameter > 0.5 mm). In fine sand (mean diameter < 0.4 mm) bottom friction becomes more important than percolation. Bottom friction depends strongly on the presence of stable sand ripples on the bottom. When the bottom is composed of silt, clay or soft organic matter, bottom motion becomes a dominant dissipation mechanism (Shemdin *et al*, 1978). In the model presented one can parameterize the percolation effect as follows:

$$D = \frac{\gamma k E}{\cos\mathrm{h}^2(kd)}, \tag{10}$$

where γ is a coefficient of permeability.

For the coarse sands and fine sands γ is equal to 1.15 cm/s and 0.124 cm/s, respectively (Shemdin *et al*, 1978).

When ocean waves encounter a current in which the surface velocity varies, an interchange energy between wave and current appears. A rate of working by surface wave motion against the mean rate of the current shear we parameterize by a formula given by Longuet-Higgins and Stewart (1961):

$$Z_{\text{current}} = -S_{\alpha\beta}\frac{\partial}{\partial x_\alpha}V_{p\beta}, \tag{11}$$

where $V_{p\beta}$ is the β component of the ocean current velocity ($\alpha = x, y$; $\beta = x, y$), $S_{\alpha\beta}$ is a radiation stress equal to:

$$\frac{c_g}{c_f}\cdot\frac{k_\alpha}{k}\cdot\frac{k_\beta}{k}\cdot E + 0.5\left(\frac{2c_g}{c_f}-1\right)\cdot\delta_{\alpha\beta}\cdot E, \tag{12}$$

where: $\delta_{\alpha\beta}$ – Kronecker's delta.

Formula (11) neglected a part of the global energy included in high-frequency band of wavy fluctuations in the water. According to Phillips (1961) this assumption is acceptable except for ocean regions with intensive wave breaking.

Propagations of surface waves are examined in the region depicted in Figure 3. We start our calculation in the region where water depth is equal

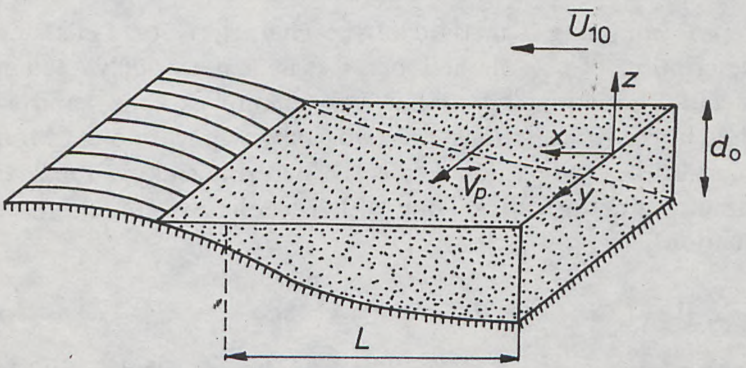

Fig. 3. The geometry of the near shore region in our model

to half of the wavelength. Values with index zero refer to the boundary of shallow water zone. Wave parameters at this point, *ie* group velocity and wavelength (or wave number), define a scale of velocity and length, respectively. We assume that all parameters describing a near shore region (bottom topography, surface current) and surface wave parameters do not vary along an axis parallel to the shore (axis y in our model) and depend only on the distance from the shore (variable x in our model).

We assume that in a near shore region water depth diminishes according to a formula: $d(x) = d_0 \exp(-Bx)$, where B characterizes a steepness of the bottom topography and the velocity of water current has a parabolic profile with a maximum value at the boundary $x = 0$.

We stop our calculations at the point where water depth is small, *ie*:

$$\frac{d}{\lambda_0} = 0.1.$$

In shallow water new effects due to nonlinear interaction between wave and bottom should be included in model equations. A method of numerical calculation does not depend on our assumptions for profiles of bottom and current. Different profiles can also be examined. It seems that in a real near shore region wave parameters should be more variable than in model presented. Especially effects of bottom and current non-homogeneity along a line parallel to the shore should be important. The present model gives only an answer to the question: to what extent do long gravity waves modify exchange processes between atmosphere and ocean in a near shore region? Our results suggest that more realistic configuration of bottom irregularities and water current should be analysed.

3. Method of calculation

We solve our problem using a method of the characteristics. Let's start from the short description of the method because it is not widely used in surface wave modelling. Equations (5) contain two unknowns k_x, k_y, and we present this method for two equations for two unknown variables. More general systems can also be studied (for details see Berezin, Zidkov, 1962). In a method of characteristics instead solving a hyperbolic system of quasi--linear partial equations, *ie*:

$$a_{ij}\frac{\partial K_j}{\partial x}+b_{ij}\frac{\partial K_j}{\partial y} = c_i; \ (\mathrm{i} = 1, 2; \ j = 1, 2), \tag{13}$$

where a_{ij}, b_{ij} are given function of x, y, K_1, K_2, we solve so-called equations of the direction of the characteristic in the form:

$$\frac{\mathrm{d}y}{\mathrm{d}x} = \lambda_i; \ (i = 1, 2) \tag{14}$$

with the differential condition on the characteristic:

$$(\lambda_i \cdot \hat{\mathbf{A}} + \hat{\mathbf{B}})\,\mathrm{d}K_1 + \hat{\mathbf{C}}\mathrm{d}K_2 + \hat{\mathbf{M}}\mathrm{d}x + \hat{\mathbf{N}}\mathrm{d}y - 0; \ (i = 1, 2), \tag{15}$$

where λ_i are the roots of the following determinant:

$$\begin{Vmatrix} b_{11} - \lambda a_{11} & b_{12} - \lambda a_{12} \\ b_{21} - \lambda a_{21} & b_{22} - \lambda a_{22} \end{Vmatrix} = 0. \tag{16}$$

Functions $\hat{\mathbf{A}}$, $\hat{\mathbf{B}}$, $\hat{\mathbf{C}}$, $\hat{\mathbf{M}}$, $\hat{\mathbf{N}}$ are defined as the following determinants:

$$\hat{\mathbf{A}} = \begin{Vmatrix} a_{11} & a_{12} \\ a_{21} & a_{22} \end{Vmatrix}; \ \hat{\mathbf{B}} = \begin{Vmatrix} b_{12} & a_{11} \\ b_{22} & a_{21} \end{Vmatrix}; \ \hat{\mathbf{C}} = \begin{Vmatrix} b_{12} & a_{12} \\ b_{22} & a_{22} \end{Vmatrix};$$

$$\hat{\mathbf{M}} = \begin{Vmatrix} c_1 & b_{12} \\ c_2 & b_{22} \end{Vmatrix}; \ \hat{\mathbf{N}} = \begin{Vmatrix} a_{12} & c_1 \\ a_{22} & c_2 \end{Vmatrix}. \tag{17}$$

Taking into account wave kinematics equations and using our assumptions for the profile of the bottom and water current, equation (15) can be rewritten as:

$$c_{gx}\frac{\mathrm{d}k}{\mathrm{d}x}x+(c_{gy}+V_p)\frac{\mathrm{d}k}{\mathrm{d}x}y = -k_y\frac{\partial p}{\partial x}-\frac{\partial \omega}{\partial d}\cdot\frac{\partial d}{\partial x}, \tag{18}$$

on the first characteristic curve $y = \text{const}$ and

$$\frac{\mathrm{d}k_y}{\mathrm{d}x} = 0 \tag{18a}$$

on second characteristic $y(x) = \int \lambda_2 \,\mathrm{d}\, x$.

For one variable problem $\hat{a}\frac{\partial E}{\partial x}+\hat{b}\frac{\partial E}{\partial y} = \hat{c}$, equations (14), (15), reduce to equations:

$$\begin{aligned} \frac{\mathrm{d}y}{\mathrm{d}x} &= \frac{\hat{b}}{\hat{a}}, \\ \frac{\mathrm{d}E}{\mathrm{d}x} &= \frac{\hat{c}}{\hat{a}}. \end{aligned} \tag{19}$$

A method of solving wave energy equation is based on formulae (19). In our problem equation (19) can be written as:

$$c_{gx}\frac{\mathrm{d}E}{\mathrm{d}x} = Z-D. \tag{20}$$

For a system of equations (5) roots of the determinant (10) are equal to $\lambda_1 = 0$ and $\lambda_2 = (c_{gy}+V_p)/(c_{gx}+U_p)$. The existence of two different roots is a precondition for using a method of characteristics.

From one boundary point of the calculated region, two curves (characteristics) given by equation (14) emerge. In a method of characteristics we find a solution of the system (5), (6) at the grid points which we find by intersection of these curves. The calculation errors depend on the grid length chosen on the boundary $x = x_0$.

This method has an advantage over other numerical methods in that we have to put initial values k_x, k_y, E at only one boundary.

Calculations are based on the Masso method. The differentials in (14) and (15) are changed into finite differences and next four linear equations for one grid points are solved. Suppose that we know wave parameters at the two neighbouring grid points (x_1, y_1) and (x_2, y_2) we can find wave parameters at the point of intersection (x_3, y_3) of the characteristics with these end points. The first two formulae, according to the Masso method, we derive from equation (14):

$$\begin{aligned} y_3 - y_2 &= \lambda_{\mathrm{II}}(x_3 - x_2), \\ y_3 - y_1 &= \lambda_{\mathrm{II}}(x_3 - x_1). \end{aligned} \tag{21}$$

Equations (21) describe intersection of characteristics at the point (x_3, y_3). The last two formulae are given by equation (15). We rewrite (15) for neighbouring points (x_1, y_1) and (x_2, y_2) and different families of the characteristics:

$$\begin{aligned} &(\lambda_{\mathrm{I}}\hat{\mathbf{A}}_1 + \hat{\mathbf{B}}_1)(k_{x_3} - k_{x_1}) + \hat{\mathbf{C}}_1(k_{y_3} - k_{y_1}) + \hat{\mathbf{M}}_1(x_3 - x_1) + \hat{\mathbf{N}}_1(y_3 - y_1) = 0, \\ &(\lambda_{\mathrm{II}}\hat{\mathbf{A}}_2 + \hat{\mathbf{B}}_2)(k_{x_3} - k_{x_2}) + \hat{\mathbf{C}}_2(k_{y_3} - k_{y_2}) + \hat{\mathbf{M}}_2(x_3 - x_2) + \hat{\mathbf{N}}_2(y_3 - y_2) = 0, \end{aligned} \tag{22}$$

where: $\hat{\mathbf{A}}_1, \hat{\mathbf{A}}_2, \ldots$ are values of the determinants (17) for points (x_1, y_1) and (x_2, y_2), respectively.
A system of equations (21), (22) allows us to find values k_{x_3}, k_{y_3} at the point (x_3, y_3) and co-ordinates of these points. In fact λ_{I}, λ_{II} depend on $k_{x_3}, k_{y_3}, x_3, y_3$ so the system (21) and (22) are not linear and the iterative method is used to avoid this complication (for details see Berezin, Zidkov, 1962). In area where λ_2 changes sign ($\lambda_2 \simeq 0$) a system of the equations (5) is not hyperbolic, and in our calculation procedure we change a system of equations when $\lambda_2 \subset (-0.1, 0.1)$. If $\lambda_2 \simeq 0$, terms of the equations (5) multiplied by $c_{gy} + V_p$ are smaller than the terms multiplied by $c_{gx} + U_p$, so after adding first of two equations (5) to the second one we have:

$$(c_{gx} + U_p)\left(\frac{\partial k_x}{\partial x} + \frac{\partial k_y}{\partial y}\right) + k_x\left(\frac{\partial U_p}{\partial x} + \frac{\partial V_p}{\partial y}\right) + k_y\left(\frac{\partial V_p}{\partial x} + \frac{\partial U_p}{\partial y}\right) = 0. \tag{23}$$

This equation with irrotational condition for wave vector number, *ie* $\frac{\partial k_x}{\partial y} = \frac{\partial k_y}{\partial x}$ constitute a new system of the equations which we solve by a method of characteristics. Precondition which enables to use this method is fulfilled because roots of the determinant (16) are equal to 0 and 1. Families of the characteristic curves are given by equations: $y = \mathrm{const}$, $y = x + \mathrm{const}_1$.
If $\lambda_2 \gg 1$ we use the same procedure as written above, only terms multiplied by $c_{gx} + U_p$ ar eliminated. Equations of the characteristics are as follows: $y = x + \mathrm{const}_2$, $x = \mathrm{const}_3$. In a case of asymptotic behaviour ($\lambda_2 \simeq 0$ or $\lambda_2 \gg 1$) calculation is also based on the system (21), (22).

One of the characteristic curves given by the system (5) $\left(y(x) = \int \lambda_2 \, \mathrm{d}x\right)$ coincides with a characteristic curve for equation (6). Using equation (20), which is satisfied for points on this curve, after solving equation (5), one can easily find energy of the long gravity waves using the method described below. If differential in equation (20) is replaced by a finite difference, we have:

$$c_{gx_{n+1,n,i}} \frac{E_{n+1,i} - E_{n,i}}{\Delta x_{n+1,n,i}} = \hat{Z} - \hat{D}, \tag{24}$$

where:
i – characteristic curve with the end point at $x = 0$, $y_{0i} = (i-1)\Delta y$,
Δy – arbitrarily chosen grid length along y axis at the boundary,
$E_{n,i}$ – wave energy at the point $(x_{n,i}, y_{n,i})$,
$E_{n+1,i}$ – wave energy at the point $(x_{n+1,i}, y_{n+1,i})$,
$\Delta x_{n+1,n,i} = \Delta x_{n+1,i} - x_{n,i}$.
Sign ˆ marks a mean value of the coefficients in equation (20) calculated as an arithmetic mean of the values at the points $(x_{n,i}, y_{n,i})$ and $(x_{n+1,i}, y_{n+1,i})$. Points $(x_{n,i}, y_{n,i})$ were found earlier by solving wave kinematics equations using a method of characteristics. These points are given as intersection points of the characteristics. Starting from boundary points $(x = 0, y_{0i})$ for which wave energy is equal to E_0, wave energy for the following grid points (on the same characteristic curve labeled by index i) is found from a linear equation (24).

4. Results

Gent and Taylor (1978) propose an interpolation formula to approximate their model predictions of the drag coefficient $C_{10} = (u_*/U_{10})^2$ in the form:

$$C_{10} = C_s(z_0, 0) + (ak)^2 F(R, c_f/u_*), \tag{25}$$

where:
$C_s(z_0, 0)$ – drag coefficient over a plane surface with the roughness parameter z_0,
ak = steepness of long gravity surface waves,
$R = -\ln(z_0 \cdot k)$,
$F(R, c_f/u_*)$ – the combined effects of direct interaction between long waves and atmosphere, and small scale exchange process due to flow modification by long wave.
In the active wave generation region (in which $8 < c_f/u_* < 12$) and for limited range of wind speed ($3 \text{ m} \cdot \text{s}^{-1} < U_{10} < 12 \text{ m} \cdot \text{s}^{-1}$) F can be taken as $R - 2.5 \cdot 10^{-3}$. For higher values of c_f/u_* F is much lower and for negative values of c_f/u_*, when the wind is against the waves, much higher value F is appropriate ($F = 10^{-2} - 10^{-3}$). We use formula (25) to find variability of C_{10} in a near shore region. In presented model input values are given at the

boundary of region where wave parameters depend on water depth. These values are as follows: $V_{p0}/C_{g0} = \{0, 0.1, 0.2, 0.5\}$, $(ak)_0 = 0.1$, $C_{g0}/u_* = \pm 30$ and $L/\lambda_0 = 100$. The last parameter expresses dimensionless width of the near shore region.

For a wave 100 m long the value of $V_{p0}/C_{g0} = 0.2$ gives a maximum velocity of the water current equal to 1.25 $m \cdot s^{-1}$. This is a resonable value. For instance, on shelf near Port Edward (South Africa) water reaches a depth of 50 m at 5 – 6 km from the shore and water current velocity is about 1.5 $m \cdot s^{-1}$ there, and decreases rapidly towards the shore (Pearce, 1977). In this case value L/λ_0 is also set correctly.

Values V_{p0}/C_{g0} close to 0.5 are representative for a shorter wave, and 0.5 is an exact value of V_{p0}/C_{g0} for wave 23 m long on the shelf near Port Edward. The value $(ak)_0 = 0.1$ can be observed in a near shore region. For waves 100 m and 20 m long this steepness implies a wave amplitude of 1.6 m and 0.32 m, respectively.

Dimensionless phase velocity equal to ± 30 characterizes wave (swell) which propagates freely at the boundary of calculated region. Energy input from wind to this wave and the other sources and sinks of the wave energy are practically negligible in this area. Waves with a value of $c_f/u_* = -30$ can appear in a near shore region as a residual of distant storm. These waves come to the shore where wind blows opposite to a direction of long waves propagation (off-shore) and waves generated by the wind do not interact with swell.

Figure 4 shows variations of wave number in a near shore region. In the case without water current wave number grows as result of reduction of water depth. As one can see from Figure 4, the role of the water current in changing wave number is secondary. A relative growth (when angle between wave direction and current is acute) and reduction of wave number (when

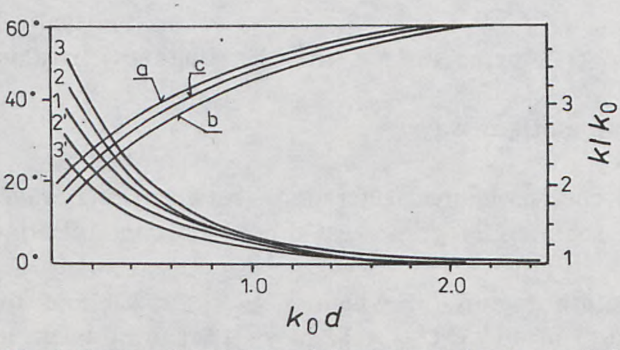

Fig. 4. Computed variations of the wave number (curves 1, 2, 2′, 3, 3′) and angle between k and line perpendicular to the beach (curves a, b, c) with dimensionless velocity of the water current V_{p0}/C_{g0}

1 – without water current, 2 – $V_{p0}/C_{g0} = 0.2$, 2′ – $V_{p0}/C_{g0} = -0.2$, 3 – $V_{p0}/C_{g0} = 0.3$, 3′ – $V_{p0}/C_{g0} = -0.3$, a – without water current, b – $V_{p0}/C_{g0} = 0.5$, c – $V_{p0}/C_{g0} = -0.5$

the angle is obtuse) reaches a maximum of 10% for current with $V_{p0}/C_{g0} = 0.1$. Correction to formula (25) depends on k^2, so interaction between surface wave and water current can be important for the analysis of an exchange procesess ocean-atmosphere, especially for strong current.

In Figure 4 is also present a change of angle between wave number vector and direction perpendicular to the shore. The angle decreases with the reduction of water depth, wave becoming more nearly perpendicular to the beach. Water current plays a little role to change this angle. For strong current the angle decreases to about 2°.

In Figure (5) we show variability of wave energy and drag coefficient as a function of dimensionless water depth ($k_0 d$). Water energy decreases in the

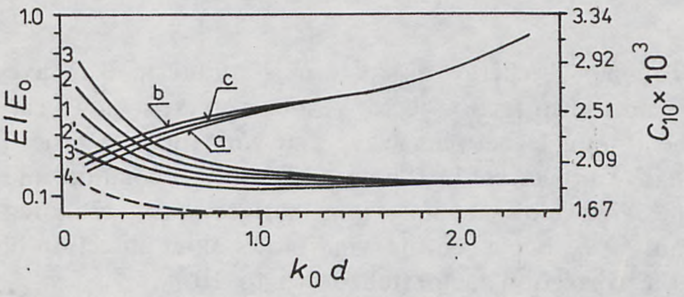

Fig. 5. Computed variations of the wave energy (curves a, b, c) and drag coefficient (curves 1, 2, 2', 3, 3', 4) with V_{p0}/C_{g0} and wave-to-wind angle
When direction of the wave propagation is opposite to the wind, notation is the same as in Figure 4. Curve 4 refers to the case when wind blows along waves and $V_{p0}/C_{g0} = 0.2$

calculated region. In the case without sources and sinks of the wave energy this is caused by changes in wave group velocity. The group velocity at first increases slightly then rapidly decreases as the water becomes more shallow, so the energy first decreases slightly before its rapid increase. When we include dissipation mechanism – percolation described by eq. (10) – in the wave energy transport equation, wave energy decreases also in a region where the group velocity increases. As the ratio of wave amplitude to the local water depth increases, the waves are deformed and appear to behave as series of solitary waves or cnoidal waves. Soon they become unstable and break. Swell tends to break when the crest-to-trough height is comparable to the local water depth. In our calculations this zone is not taken into account.

Energy dissipation due to percolation effectively changes wave energy (Fig. 6). When bottom material consists of coarse sand, characterized by coefficient of permeability $\gamma = 2\ \mathrm{cm \cdot s^{-1}}$, wave energy decays abruptly in shallow water, so near the beach the correction factor in formula (25) is about 2% of the value of $C_s(z_0, 0)$. In this case the other model parameters are as follow: $V_{p0}/C_{g0} = 0.1$ and $L/\lambda_0 = 100$. When bottom material consists

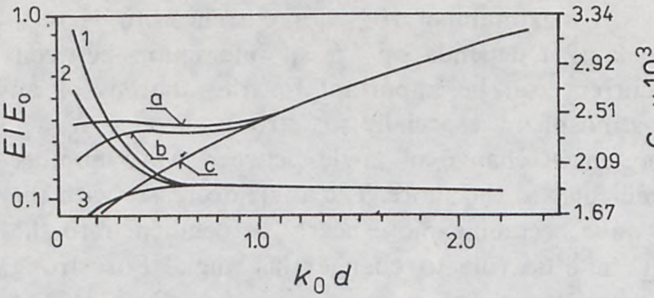

Fig. 6. The role of bottom material in variations of the wave energy (curves a, b, c) and drag coefficient (curves 1, 2, 3); for $V_{p0}/C_{g0} = 0.1$ a and $1-\gamma = 0.1\ \mathrm{cm \cdot s^{-1}}$ (coefficient of permeability), b and $2-\gamma = 0.5\ \mathrm{cm \cdot s^{-1}}$, c and $3-\gamma = 2\ \mathrm{cm \cdot s^{-1}}$

of fine sand and $\gamma = 0.1\ \mathrm{cm \cdot s^{-1}}$ energy dissipation is quite small. Wave energy decreases slowly and the correction factor is much greater. As we can see from Figures (5) and (6), angle between wave and wind plays a crucial role in momentum exchange processes. In the case without percolation and water current, when the wind blows against long surface wave, the drag coefficient increased about $60^0/_0$, but when the wind blows along direction of the wave propagation the correction factor fall down to $10^0/_0$.

When the angle between waves and water current is acute, growth of the wave number is greater than in the case when the angle is obtuse. In the first case $-k_y \frac{V_p}{x} > 0$ (in the second case < 0) and the rate of growth k_x is larger than in the second case – see equation (18).
According to formula (25), the drag coefficient in the first case is greater than in the second case. For $V_{p0}/C_{g0} = -0.2$ and $\gamma = 0$ maximum corrections are $40^0/_0$ of the value of $C_s(z_0, 0)$. It is about $50^0/_0$ of the correction for the case when $V_{p0}/C_{g0} = 0.2$. For greater values of $(ak)_0$ and $|V_{p0}/C_{g0}|$ this difference is more distinctive.

An energy flux to the wave due to water current-wave interaction practically do not change wave energy (Fig. 5). Mean shear of water current in our model is quite small. A coefficient characterizing the efficiency of sources (sinks) *ie* $E^{-1}\,\mathrm{d}E/\mathrm{d}t$ is of the order of 10^{-4}. In shallow water zone it is comparable to a dumping coefficient due to percolation in fine sand. As we can see, only a change in the wave kinematics caused by water current is important for momentum exchange process.

In our model energy input from the wind is not decisive for wave energy. A width of the calculated part of the near shore region is small *ie* $L/\lambda_0 = 100$, whereas a length scale for change of wind driven wave is about thousands of wavelengths. For a wider near shore region and for a smaller value of $|c_f/u_*|$ the wind-wave interaction should become more important.

5. Conclusions

The following conclusions can be drawn from our study:

(i) Changes of long surface wave parameters in a near shore region influence momentum transfer between the atmosphere and ocean.

(ii) In a near shore region, which is homogeneous along an axis parallel to the beach, the sea-atmosphere interaction increases as the water becomes more shallow.

(iii) When the wind blows opposite to the direction of wave propagation, the sea-atmosphere interaction intensifies. For steep gravity waves the role of low-frequency band of wave spectrum in momentum transfer between the atmosphere and ocean (A-O) is comparable to the role of high-frequency surface irregularities (these components define roughness of the sea surface)

(iv) Water current and type of the bottom material influence exchange process A-O. The first factor changes mainly kinematics of the wave train, the second dynamics.

(v) A numerical method of characteristics applied to kinematics and wave energy equations is fast and accurate.

References

Berezin I. S., Zidkov N., 1962, *Metody vychislenii*, Izdat. Fiziko-Matematicheskoi Literatury, Moskva.

Druet C., Siwecki R., 1984, *The influence of early stages of development of wind waves on the effective roughness of the water free surface*, Oceanologia, 18.

Gent P. R., 1977, *A numerical model of the air flow above water waves*, Fluid. Mech., 82.

Gent P. R., Taylor P., 1978, *A numerical investigations of variations in the drag coefficient for air flow above water waves*, Q. Royal Meteorol. Soc., 104.

Haase L., Gruenewald M., Hasselmann D. E., 1978, *Field observations of air flow above the waves*, Proc. NATO Conf. on Turbulent Fluxes through the Sea Surface, Wave Dynamics, and Prediction, Plenum Press, New York.

Kitaigorodskii S. A., 1970, *Fizika vzaimodeistviya atmosfery i okeana*, Gidrometeoizd., Leningrad.

Kuznetsov O. A., 1978, *Rol' vysokochastotnykh gravitatsionnykh voln v aerodinamicheskom soprotivlenii morskoi poverkhnosti*, Okeanologiia, XVIII, 2.

Longuet-Higgins M. S., Stewart R. W., 1961, *The changes in amplitude of short gravity waves on steady no-uniform current*, J. Fluid Mech., 10.

Massel S., Druet C., 1980, *Spectra of wind waves in coastal zone*, Rozp. Hydrotech., 41.

Munk W., 1955, *Wind stress on water, an hypothesis*, Q. J. Royal Meteorol. Soc., 349.

Pearce A. F., 1977, *Some features of the upper 500 m of the Agulhas current*, J. Mar. Res., 35.

Phillips O. M., 1961, *A note on the turbulence generated by gravity waves*, J. Geophys. Res., 66.

Shemdin O., Hasselmann K., Hsiao S. V., Herterich K., 1978, *Non-linear and linear bottom interaction effects in shallow water*, Proc. Conf. on Turbulent Fluxes through the Sea Surface, Wave Dynamics, and Prediction, Plenum Press, New York.